Simple Shear and "Turbulence" of Polycrystals

Yan Beygelzimer
Donetsk Physics and Technology Institute
Ukrainian National Academy of Sciences
72 R. Luxembourg St., Donetsk, 83114, Ukraine

November 11, 2008

Abstract

We present an analogy between large plastic deformations of polycrystals and turbulent flows in fluid dynamics. The analogy explains a number of effects observed during large deformations, still unexplained in the language of plasticity theory. We also propose a phenomenological criteria characterizing the "turbulence" of polycrystals. Using this criteria, the paper shows that simple shear is possible only in materials whose representative elements admit a non-symmetric component of the corresponding velocity gradient. If this condition is not satisfied, the material only imitates simple shear replacing it with pure shear.

Keywords: Large plastic deformation, turbulence, simple shear, pure shear, severe plastic deformation, analogy, microstructure

1 Introduction

There are many unanswered questions on the border between the mechanics of large plastic deformations and materials science. For example, why do upsetting and torsion tests often share a universal stress-strain curve under a relatively small equivalent strain, while when the strain is large, these curves diverge sharply? Why does hardening saturate after several passes of equal-channel angular pressing (ECAP) and twist extrusion (TE), while subsequent rolling and direct extrusion increase the yield stress? Why after multiple ECAP or TE passes, does metal ductility cease to decline and even go up? Why don't we see micropores in submicrocrystalline materials obtained using Severe Plastic Deformation (SPD) methods, while such inhomogeneities are present in materials that underwent the same strain via other methods? Finally how do we distinguish severe from large plastic deformations?

We believe that such questions can be answered using an analogy of large plastic deformations of polycrystals with turbulence in fluid dynamics. This is what the paper is about.

2 The Basic Idea

As shown theoretically [1, 2] and experimentally [3, 4], the internal stress emerging when a polycrystal undergoes plastic deformation, causes bends and shifts in the crystal lattice—a process that can be described using a random vortex displacement field. For a certain value of lattice curvature, it becomes energy-efficient for a disorientation boundary to appear, decreasing the elastic energy of the crystal. The latter energy partially transforms into the elastic energy of the newly formed smaller fragments and into the surface energy

of their boundaries. A portion of it dissipates when the fragments adjust to their neighborhood. In addition, relative orientations of the elements gradually penetrate lower-lying scales, which creates progressively smaller pulsations in the random vortex displacement field. Sliding along deformation boundaries causes the grain refinement process to stop once the fragment size becomes sufficiently small [5]. The smallest fragment size for a given material is determined by deformation conditions (e.g., deformation scheme, strain rate, temperature, hydrostatic pressure).

This view resembles the development of turbulence in fluids, when large-scale vortices lose their stability creating smaller-scale vortices. The kinetic energy transfers from large-scale to lower-scale levels until it reaches the smallest scale where it dissipates due to viscosity [6]. The difference between the grain refinement process and turbulence is that instead of kinetic energy we have the elastic potential energy of a polycrystal.

This connection between polycrystal grain refinement and turbulence in fluids goes back to Taylor [7], who pointed out that in both cases there originate random strain and displacement fields, which are characterized by the presence of pulsations on different scales. This is evidenced by microstructures of deformed polycrystals [8, 9] whose random structures resemble turbulent flows in fluids [10].

A strong evidence in support of the analogy is the deformation-induced intermixing of different phases and inclusions [9]. This effect is one of the most important manifestations of a turbulent flow and is explained by active mixing [6]. Figure 2 shows microstructures of phosphorous-copper alloy (8.5 mass % of P) and secondary aluminum alloy (silumin, 6-8 mass % Si) before and after two passes of twist extrusion. It is clear that twist extrusion leads to intense grain refinement and erosion of large inclusions of the α-phase into the phosphorous-copper alloy (Figure 2a and b) and eutectic second-phase particles in the silumin (Figure 2c and d).

The described analogy allows one to apply several ideas which proved to be useful in investigating turbulence, to describing plastic deformations and fracture. One such idea is the structural self-similarity of random strain and displacement fields. For example, Barenblatt [13] uses the assumption of self-similarity of a microcrack ensemble to describe the process of multiple-point fracture. As another example, the self-consistent model for polycrystals proposed in [12] is a cellular automata with a self-similar structure. This allowed the authors to account for the multi-level structure of the material introducing the notion of a fractal yield surface. The latter revealed an additional connection between micromechanical models of polycrystals and the phenomenological theory of plasticity. Finally, the model of metal grain refinement and fracture proposed in [5] is based on the assumption of self-similarity of a high-angle boundary net and the limiting fragment size. The results in [5] will be used substantially in this paper.

The following sections present several new observations about large plastic formations based on the analogy above.

3 A phenomenological parameter characterizing the "turbulence" of polycrystals

Let us introduce a dimensionless parameter that, in some precise sense, is analogous to the Reynolds number and can characterize the turbulence of polycrystals. The Reynolds number is essentially the ratio of kinetic energy per unit fluid volume to specific dissipation energy. Consequently, it quantifies the effectiveness of a given fluid in dissipating the supplied energy. The analogous parameter of a polycrystal has the following form:

$$R' = \frac{\text{stress energy}}{\text{dissipation energy}}. \tag{1}$$

Considering relation (1) for uniaxial tension, for an infinitely small time interval dt, we get

$$R' = \frac{\sigma_u(\dot{e}_{el} + \dot{e})dt}{\sigma_u \dot{e}_p dt} = 1 + \frac{1}{E}\frac{d\sigma_u}{de_p} \tag{2}$$

where σ_u is the true stress, $\dot{e}_{el}$ and $\dot{e}_p$ are the elastic strain rate and the plastic deformation rate respectively, and E is the Young modulus.

Expression (2) should be viewed as indicating that the coefficient of strain hardening $\frac{d\sigma_u}{de_p}$ (which is successfully used for identifying strain hardening stages [14, 15]) can characterize the "turbulence" build-up in a polycrystal.

During grain refinement, a high-angle boundary net starts to grow in a self-similar fashion [5]. When the strain is e_{p_2}, the geometric pattern of the boundary ensemble is the same as that at e_{p_1}, only scaled by a factor of $f = f(\frac{e_{p_2}}{e_{p_1}})$. The scaling function should satisfy the obvious condition $f(\frac{e_{p_3}}{e_{p_1}}) = f(\frac{e_{p_2}}{e_{p_1}})f(\frac{e_{p_3}}{e_{p_2}})$, which implies that $f \sim (\frac{e_{p_2}}{e_{p_1}})^m$, and thus the average grain size is a function of e_p. Taking into account the Hall-Petch relation, σ_u is a power function of e_p during grain refinement:

$$\sigma_u \sim e_p^n. \tag{3}$$

Thus we can take

$$R = \left(\frac{1}{\sigma_u}\frac{d\sigma_u}{de_p}\right)^{-1}. \tag{4}$$

as the dimensionless parameter quantifying the "turbulence" of a polycrystal (i.e., the intensity of high-angle boundary formation). Indeed, from (3) and (4), under intense formation of high-angle boundaries, parameter R has an intermediate asymptotics of

$$R \sim \frac{1}{n}e_p. \tag{5}$$

Thus the interval $\lfloor e_{p_1}, e_{p_2} \rfloor$, where $R(e_p)$ has intermediate asymptotics (5), corresponds to the stage of intense grain refinement. Figure 1 shows a typical dependence for $R(e_p)$. According to [5], increasing R when $e_p > e_{p_2}$, with a departure from a linear dependence, points to the fact that grain refinement fades due to sliding along high-angle boundaries.

Relations (2) and (4) assume a simple uniaxial deformation. For an arbitrary stress-strain state, σ_u should be the intensity of the strain deviator, and e_p the equivalent strain. Thus according to (4), in order to compute R for an arbitrary deformation process, we need to experimentally obtain $\sigma_u(e_p)$. To do that, we need to determine the value of σ_u after each deformation pass. This can be done using either the yield stress YS or the Vickers hardness number (HV) of the specimen. The first method is based on the von Mises plasticity condition according to which $\sigma_u = \mathrm{YS}$. The second is based on $(\sigma_u - \mathrm{HV})$ (which is the same for all strain states) and a calibration curve obtained, for example, using upsetting test experiments. With a sufficiently high precision, metals that underwent a strain of at least 0.3-0.4, have a linear dependence between σ_u and HV [16]. In this case, we can take

$$R = \left(\frac{1}{\mathrm{HV}}\frac{d\,(\mathrm{HV})}{de_p}\right)^{-1}. \tag{6}$$

Figure 3b plots $R(e_p)$ for titanium BT1-0, based on the experimental dependence of its yield stress YS on the strain rate in Twist Extrusion (TE) (Figure 3a). Recall that according to the von Mises plasticity condition, $\sigma_u = \mathrm{YS}$. The equivalent strain e_p in TE was obtained using a numerical method described in [16]. In agreement with a previous discussion, the dependence in Figure 3b shows that the most intense formation of high angle boundaries under TE occurs when the equivalent strain is 1.5-3.5, which corresponds to passes two to four.

4 On simple shear and its imitation

In mechanics, a simple shear is a deformation process defined by the velocity field

$$V_1 = kx_2, \quad V_2 = V_3 = 0. \tag{7}$$

Such a field is realized, for example, for a laminar flow of fluid between two parallel blades moving relative to each other.

The velocity gradient corresponding to field (7) has a symmetric and a non-symmetric component. The symmetric component characterizes the strain rate, the non-symmetric—the rotation rate. Indeed, plugging (7) into a well-known decomposition of the velocity gradient

$$\frac{\partial V_i}{\partial x_k} = \frac{1}{2}\left(\frac{\partial V_i}{\partial x_k} + \frac{\partial V_k}{\partial x_i}\right) + \frac{1}{2}\left(\frac{\partial V_i}{\partial x_k} - \frac{\partial V_k}{\partial x_i}\right) = \dot{e}_{ik} + \omega_{ik}, \tag{8}$$

we get

$$\dot{e}_{12} = \dot{e}_{21} = 0.5k, \quad \omega_{12} = -\omega_{21} = 0.5k. \tag{9}$$

The j-th component of the vorticity can be determined using the formula (see, for example, [17])

$$(\mathrm{rot}\,\vec{V})_j = \epsilon_{jki}\omega_{ik}. \tag{10}$$

For the rotation velocity, the corresponding formula is

$$\Omega_j = \frac{1}{2}(\mathrm{rot}\,\vec{V})_j = \frac{1}{2}\epsilon_{jki}\omega_{ik}. \tag{11}$$

Plugging relations (9) into (10) and (11), we get the following non-zero vorticity and rotation velocity components:

$$(\mathrm{rot}\,\vec{V})_3 = -k, \quad \Omega_3 = -0.5k. \tag{12}$$

According to (12), each material point of the specimen has a non-zero vorticity. The main assumption of continuum mechanics is that a material point is a representative volume element (RVE) of the material, containing a large number of its structural elements. Taking this assumption into account, let us see what requiring a non-zero vorticity implies in relation to an RVE.

Imagine describing an arbitrary contour Γ around any material point. Stokes' theorem (see, for example, [17])

$$\oint_\Gamma V_\tau dl = \int_S (\mathrm{rot}\,\vec{V})_3 dS \tag{13}$$

and relation (12) imply that the contour integral on the left equals $-kS$. Contract the contour to the considered material point and shift to a lower scale where the RVE already has some internal structure. (See Figure 4 for a schematic illustration.) During plastic deformation, a velocity field $\vec{\nu}$ is formed inside the RVE. Applying Stokes' theorem to this field and using the obvious fact $\oint_\Gamma \nu_\tau dl = \oint_\Gamma V_\tau dl = -kS$, we get

$$\int_S (\mathrm{rot}\,\vec{\nu})_3 dS = \oint_\Gamma \nu_\tau dl = -kS.$$

This relation implies the following expression for the expected value of a vorticity component inside the RVE:

$$\langle (\mathrm{rot}\,\vec{\nu})_3 \rangle = -k, \tag{14}$$

where $\langle\cdot\rangle$ denotes the expectation across the RVE volume. The RVE can't rotate as a whole. So for relation (14) to hold, we need structural elements to rotate with an average rate of $\langle\omega_3\rangle = -0.5k$. This is what distinguishes simple shear from pure shear. For pure shear, analogous arguments give $\langle\omega_3\rangle = 0$.

Distributed rotations of structural elements are possible only under grain refinement or free sliding along high angle boundaries. If neither condition is satisfied, rotations are blocked at the macro-level, in which case we are left with only the symmetric component of the velocity gradient corresponding to pure

shear (also known as flat lengthening). This is a fundamental fact that is ignored in the classic plasticity theory, which does not distinguish between simple and pure shears. Until structural elements can freely rotate in the representative volume (in every "material point" in the language of continuum mechanics), the body can only imitate simple shear. (A "material point" does not provide the necessary value of the non-symmetric component, i.e., vortex.) Thus, when grain refinement is not sufficiently developed and distributed rotations of structural elements are hindered, an attempt to implement a simple shear accomplishes only flat lengthening.

As grain refinement advances, forming high-angle boundaries which facilitate rotations, the non-symmetric component of the velocity gradient increases, and the deformation gradually approaches simple shear. The latter executes only when structural elements are completely free to rotate, which happens when grain refinement (formation of new boundaries) stops and the solid body becomes ideally plastic (i.e., strain hardening is lost).

Figure 5a shows our installation for simple shear in the longitudinal center plane of a cylindrical specimen (developed with a graduate student, Roman Kulagin). The core part consists of two deforming inserts (1) with semi-cylindrical cutouts that form the specimen enclosure. The inserts are placed into the casings (2). The inserts (3) allow one to specify the initial shift of the two casings with respect to each other. The assembled package is then placed into the housing (4) of the same height as the casings (2). Since the casings are initially shifted with respect to each other, the end face of one juts out of the housing. This installation is placed inside a thick-walled cylindrical container (not shown), situated on the press. The diameter of the inner channel of the container equals the diameter of the circle described around the cross-section of the housing. The end face of the installation is pressed with a plunger of the same diameter as the diameter of the channel. This induces a relative shift of the casings (2), deforming the specimen (see Figure 5b).

The container has two functions. First, it holds the installation strictly vertical. Second, it can hold hydraulic fluid, allowing us to implement a shift under pressure. This option is intended for a future investigation of the effect of strain on simple shear.

Figure 5b makes it seem as if the specimen underwent a simple shear along the longitudinal center plane. However, the grid plotted on the specimen before the deformation shows that the latter is not a simple shear but, as strain increases, it approaches simple shear and becomes more and more localized near the longitudinal center plane. (The experiment was performed with Roman Kulagin.)

It is probably appropriate to introduce a special term for continuous mediums that allow a non-zero vortex in each material point. Examples of such a medium are models of different fluids, powders, and submicrocrystalline materials obtained via SPD methods.

Using the parameter R above, a simple shear is realized when $R \to \infty$. For practical purposes, a simple shear is realized with a sufficient freedom of rotation with fragment sliding, when grain refinement is starting to die out. In the case of TE of titanium, for example, simple shear occurs when $R > 20$ (see Figure 2b).

The fact that simple shear does not depend on the rotation value (i.e., strain) under a constant pressure level, supports the absence of strain hardening during simple shear (see Figure 7). This means that the properties of any material realizing such shear should not depend on the strain, i.e., the material should be ideally plastic. If viscous strengthening is absent as well, the material loses its stability, and the shear is realized within a narrow band [5].

The above view explains a number of effects observed during simple shear, including the following:

1. A universal stress-strain curve in upsetting (lengthening) and torsion tests under a relatively small equivalent strain, and a sharp divergence of these curves when the equivalent strain is large [18, 19]. Since simple shear is impossible under small equivalent strain, torsion turns into a simple lengthening of the specimen fibers. When the equivalent strain is large, however, a simple shear is realized, with a characteristic saturation of hardening of the deformed material.

2. Distortion of the specimen surface during torsion [19], explained by the fact that material fiber lengthening (at a 45° angle to the shear plane) leads to lengthening of the entire specimen when rotations are limited, while the distance between plungers remains constant.

3. Formation of "rollers" during shear (e.g., wear debris formed during friction).

4. A slow-down of grain refinement and saturation of metal hardening after several passes of equal-channel angular pressing (ECAP) and twist extrusion (TE). The feasibility of further grain refinement with hardening via a subsequent rolling or direct extrusion [21, 22].

5. A continuing increase in fragment disorientation angles with an increase in strain under TE, while fragment size is already constant [23].

The last two effects are explained by the fact that, after sufficiently many passes, ECAP and TE realize simple shear without strain hardening, with the ceasation of grain refinement, and with fragments free to rotate. The way the rotations are carried out is not purely mechanical (i.e., as a rotation of rigid balls with a simultaneous sliding along the boundaries), but rather via the formation of a self-replicating structure (in the statistical sense). As mentioned earlier, the main distinguishing characteristic of the structure, from the viewpoint of mechanics, is the ability to provide a non-zero non-symmetric component of the velocity gradient (vortex) in the representative volume element (RVE). This is precisely why materials with such a structure can undergo large deformations without getting fractured, i.e., have high ductility (see Section 5).

We conclude with a comment about calculating strain for torsion under pressure. Two formulas are currently used in the literature [24]. The first is based on calculating logarithmic strain under fiber lengthening; the second—on viewing this process as a simple shear. According to the above, to calculate strain in this case we need an expression that would coincide with the first formula under small values of R, and as R increases, would gradually turn into the second formula.

5 Strain Induced Porosity

As remarked in the beginning of Section 2, plastic deformation of polycrystals forms a random microstrain field. We analyzed only one related effect, namely the emergence of a random vortex displacement field. Another effect is strain induced porosity that decreases metal ductility [5, 25, 26, 27]. A high hydrostatic pressure heals some of the inhomogeneities, thereby slowing down the decrease in ductility. Ref. [5] proposes a mathematical model describing this process.

According to [5], the change in the total volume of inhomogeneities during plastic deformation under pressure is due to conflicting processes of formation and healing. The intensity of formation decreases with an increase in the area of high angle boundaries since the latter allow for a relaxation of microstrains via intergrain sliding. In the limit, when a metal forms a structure providing it with ideal plasticity, inhomogeneities cease formation and the healing process leads to their total disappearance.

From the discussion in Section 3, the processes increasing metal ductility have to occur when $e_p > e_{p_2}$ (see Figure 1). Figure 8 shows how relative neck tightening during tearing of titanium specimen depends on the strain value in TE. (Processing conditions are the same as in Figure 3.) A comparison of the plots in Figure 3b and Figure 8 supports the proposed hypothesis. Specimen ductility was evaluated using relative neck tightening during tearing instead of relative lengthening before neck formation. In the absence of viscous strengthening, ductility characterizes the intensity of strain hardening, which obviously decreases with strain.

The proposed hypothesis also explains why submicrocrystalline materials obtained using SPD methods don't show any micro-inhomogeneities, unlike materials that underwent the same strain via other methods (as confirmed using high-precision density measurements, electronic microscopy and X-rays; see, for example, [28, 29]). This happens because as creation of micro-inhomogeneities attenuates, the healing process leads to their gradual disappearance with subsequent deformation passes.

6 Conclusions

1. There is a fruitful analogy between large plastic deformations of polycrystals and turbulence of fluids. Ultrafine grained structures and nanostructures obtained using SPD methods can be viewed as a "frozen turbulence" of polycrystals.

2. As a dimensionless parameter characterizing the turbulence of polycrystals we can take $R = \left(\frac{1}{\sigma_u}\frac{d\sigma_u}{de_p}\right)^{-1}$ or $R = \left(\frac{1}{\mathrm{HV}}\frac{d(\mathrm{HV})}{de_p}\right)^{-1}$.

3. Simple shear is possible only in materials whose representative elements admit a non-symmetric component of the corresponding velocity gradient. For polycrystals, this means the ability of fragments to rotate freely due to sliding along the boundaries between them, i.e., the absence of grain refinement and strain hardening. Using the parameter R above, a simple shear is realized when $R \to \infty$. For practical purposes, as grain refinement dies out, sufficient freedom of rotation exists for simple shear to occur. In the case of TE of titanium, for example, simple shear occurs when $R > 20$.

4. After sufficiently many passes, ECAP and TE realize simple shear without strain hardening, with the ceasation of grain refinement, and with fragments free to rotate. The way the rotations are carried out is not purely mechanical (i.e., as a rotation of rigid balls with a simultaneous sliding along the boundaries), but rather via the formation of a self-replicating structure (in the statistical sense). As mentioned earlier, the main distinguishing characteristic of the structure, from the viewpoint of mechanics, is the ability to provide a non-zero non-symmetric component of the velocity gradient (vortex) in the representative volume element (RVE).

References

[1] G. I. Taylor. Plastic Strain in Metals. Journal of the Institute of Metals 62, 307–324 (1938)

[2] R. J. Asaro. Crystal Plasticity. Trans. ASME, Ser. E, J. Appl. Mech 50 (4b), 921–934 (1983)

[3] T. E. Konstantinova, V. B. Primisler and A. A. Dobrikov. Bending of a crystal lattice as an independent form of plastic deformation, Met. Phys. Adv. Tech 16, 1191–1201 (1997)

[4] A. N. Tyumentsev, Yu. P. Pinzhin, M. V. Tretjak, A. D. Korotaev, I. A. Ditenberg, R. Z. Valiev, R. K. Islamgaliev, A. V. Korznikov. Evolution of defect substructure of metal alloys at microscopic and mesoscopic level under torsion. Theoretical and Applied Fracture Mechanics 35, 155–161 (2001)

[5] Y. Beygelzimer. Grain refinement versus voids accumulation during severe plastic deformations of polycrystals: A mathematical simulation, Mechanics of Materials, Vol. 37, No. 7, 753–767 (2005)

[6] A.S. Monin, A. M. Yaglom. *Statistical hydromechanics*. Saint-Petersburg, Hydrometeoizdat, 696 pages (1992)

[7] G.I. Taylor. Strain in crystalline aggregates. Proceedings of the Colloquium on Deformation and Flow of Solids (Madrid, 1955). Berlin: Springer, 3–12 (1956)

[8] R. Z. Valiev and T.G. Langdon. Principles of equal-channel angular pressing as a processing tool for grain refinement. Progress in Materials Science, Vol. 51, No. 7, 881–981 (2006)

[9] Y. Beygelzimer, V. Varyukhin, S. Synkov, and D. Orlov. Useful properties of twist extrusion. Materials Science and Engineering A xxx xxx-xxx, doi:10.1016/j.msea.2007.12.055 (2008)

[10] Milton Van Dyke (editor). An Album of Fluid Motion, The Parabolic Press, Stanford, CA (1982)

[11] G. I. Barenblatt. Scaling, self-similarity, and Intermediate Asymptotics. Cambridge University Press, 386 pages (1996)

[12] Y. Beygelzimer and A. Spuskanyuk. The thick yield surface: An idea and approach for investigating its structure. Philosophical Magazine A, Vol. 79, No. 10, 2437–2459 (1999)

[13] W. Nix, J. Gibeling, D. Hugher. Time-dependent deformation of metals, Metallurgical Transactions A, Vol. 16, No. 12, 2215–2226 (1985)

[14] Yu. N. Podrezov. Structural sensitivity of mechanical properties of nanomaterials, Physics and Technics of High Pressures, Vol. 14, No. 4, 42–52 (2004)

[15] G. D. Del. Determining pressure in a plastic region using hardness distribution. Manufacturing Engineering (in Russian), Moscow, 199 pages (1971)

[16] Y. Beygelzimer, A. Reshetov, S. Synkov, O. Prokof'eva, and R. Kulagin. Kinematics of Metal Flow during Twist Extrusion Investigated with a New Experimental Method. Journal of Materials Processing Technology, DOI 10.1016/j.jmatprotec.2008.08.022

[17] J. E. Marsden, A. J. Tromba. Vector Calculus (5th edition). W. H. Freeman & Co, New York (2003)

[18] D. F. Bell. Experimental foundation of solids mechanic. In Flugge, S. (Ed.), The Encyclopedia of Physics, vol. VIa/ 1. In: Trusdell, C. (Ed.), Mechanics of Solids 1. Springer-Verlag, Berlin, 430 pages (1973)

[19] P. W. Bridgman P.W. Studies in Large Plastic Flow and Fracture with Special Emphasis on the Effects of Hydrostatic Pressure. New York-Toronto-London, 440 pages (1952)

[20] P. W. Bridgemen. Studies in Large Plastic Flow and Fracture, McGrawHill, New York (1952)

[21] V. V. Stolyarov, Y. T. Zhu, I. V. Alexandrov, T. C. Lowe, R.Z. Valiev. Grain refinement and properties of pure Ti processed by warm ECAP and cold rolling. Materials Science and Engineering A 343, 43–50 (2003)

[22] V. Stolyarov, Y. Beygelzimer, D. Orlov, and R. Valiev. Refinement of Microstructure and Mechanical Properties of Titanium Processed by Twist Extrusion and Subsequent Rolling. The Physics of Metals and Metallography, Vol. 99, No. 2, 204–211 (2005)

[23] D. Orlov, Y. Beygelzimer, S. Synkov, V. Varyukhin and Z. Horita. Evolution of Microstructure and Hardness in Pure Al by Twist Extrusion. Materials Transactions, Vol. 49, No. 1, 2–6 (2008)

[24] R. Z. Valiev and I. V. Alexandrov. Voluminous nanostructured metals: manufacturing, structure, and properties. AcademKniga, 398 pages (2007)

[25] F. A. McClintock. A criterion for ductile fracture by the growth of holes. Trans ASME, J. Appl. Mech. 17, 363 (1968)

[26] V. L. Kolmogorov. On the history of the determination of ductile fracture (ductility) of metals. Journal of Materials Processing Technology 70, 190–193 (1997)

[27] Y. E. Beygelzimer, B. M. Efros, V. N. Varyukhin, A. V. Khokhlov. Continuum model of the structurally-inhomogeneous porous body and its application for the study of stability and viscous fracture of materials deformed under pressure. Engineering Fracture Mechanics 48 (5), 629–640 (1994)

[28] S. V. Smirnnov, V. I. Levit, A. A. Bogatov, V. L. Kolmogorov, A. V. Shalimova. Damage in Drawing a Wire of Low-Carbon Steel. Russ. Metall 2, 147–153 (1987)

[29] P. G. Cheremskii, V. V. Slezov, V. I. Betekhtin. Pores in a solid body. Energoatomizdat, 376 pages (1990)

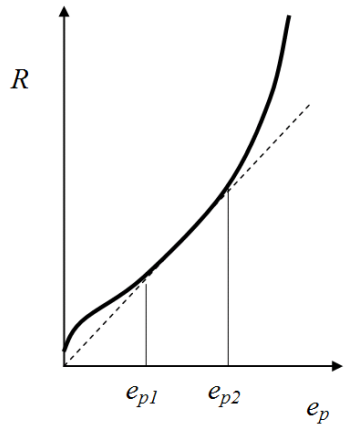

Figure 1: The nature of the $R(e_p)$ dependence. The interval between e_{p_1} and e_{p_2} corresponds to intense formation of high-angle boundaries.

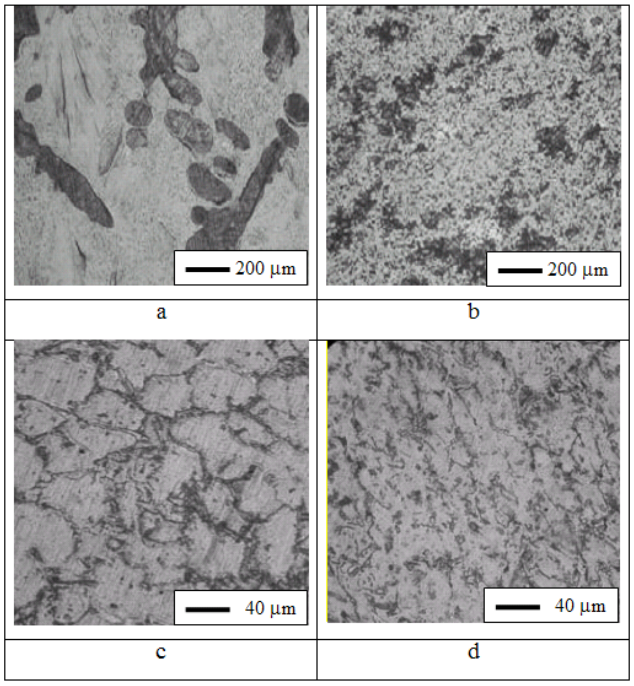

Figure 2: Microstructures of phosphorous-copper alloy (8.5 mass % of P) (a,b), and secondary aluminum alloy (silumin, 6-8 mass % Si) (c,d) before (a,c) and after (b,d) two passes of twist extrusion. Deformation temperature T=1000C, backpressure P=200 MPa.

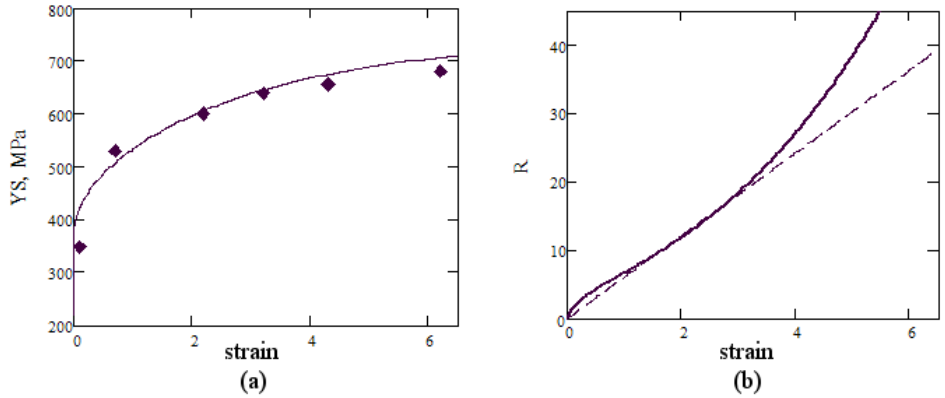

Figure 3: Dependence of the yield stress (a) and parameter R (b) on the strain rate during titanium (BT1-0) deformation using TE. Deformation temperature 400° C, anti-pressure 200 MPa, extrusion die with cross-section size 28×18 mm and twist line pitch angle of 45° and 55°. TE was performed as described in [16]. Experiment performed with A. V. Reshetov, O. V. Prokof'eva, and R. Y. Kulagin.

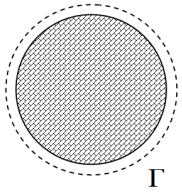

Figure 4: A diagram of an RVE with integration contour Γ.

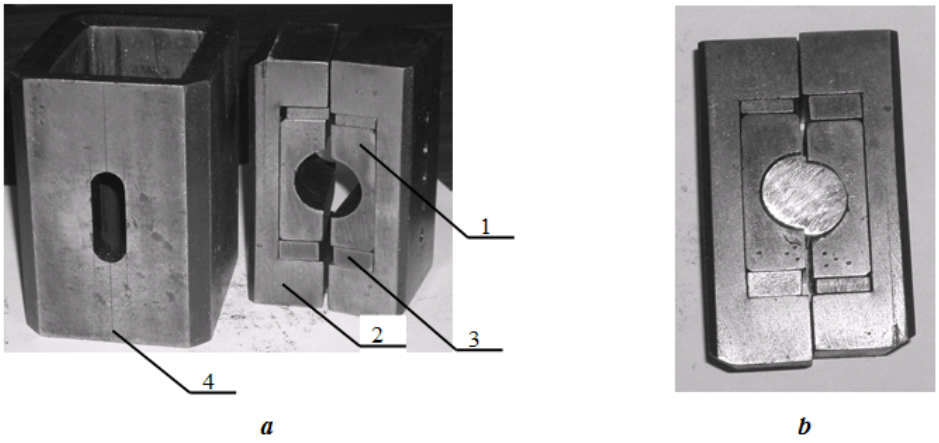

Figure 5: (a) Our installation for simple shear in the longitudinal center plane of a cylindrical specimen; (b) the specimen after shift (see text for details)

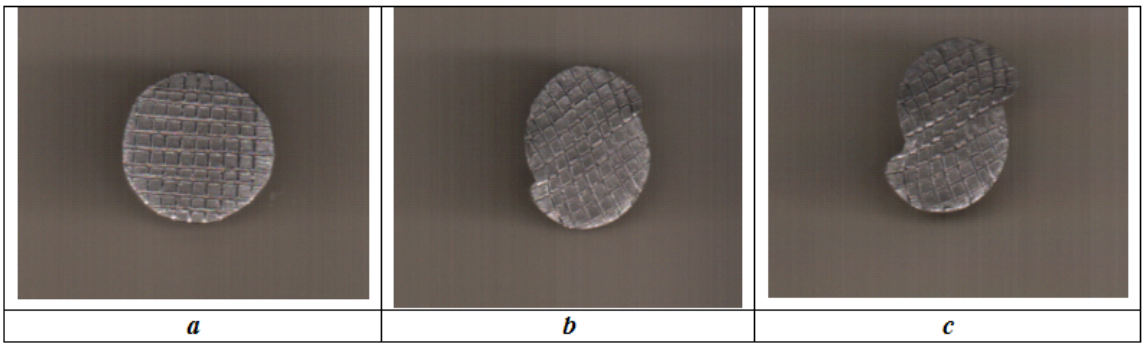

Figure 6: The specimen's grid before (a) and after (b,c) the deformation; (b) and (c) correspond to two different strain levels.

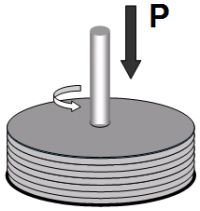

Figure 7: A diagram showing that simple shear under constant pressure P is invariant to rotation.

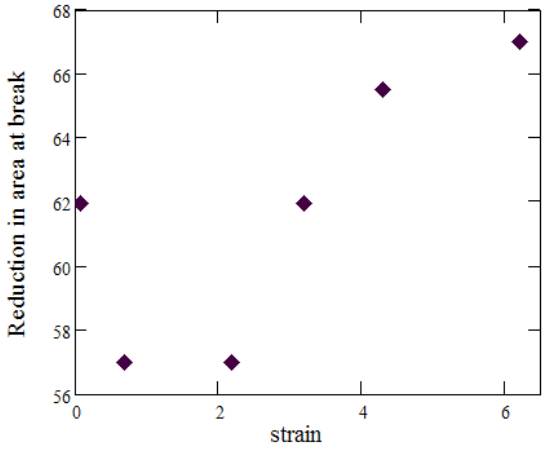

Figure 8: Dependence of relative neck tightening during tearing from strain rate in TE. (Processing conditions are the same as in Figure 3.)